

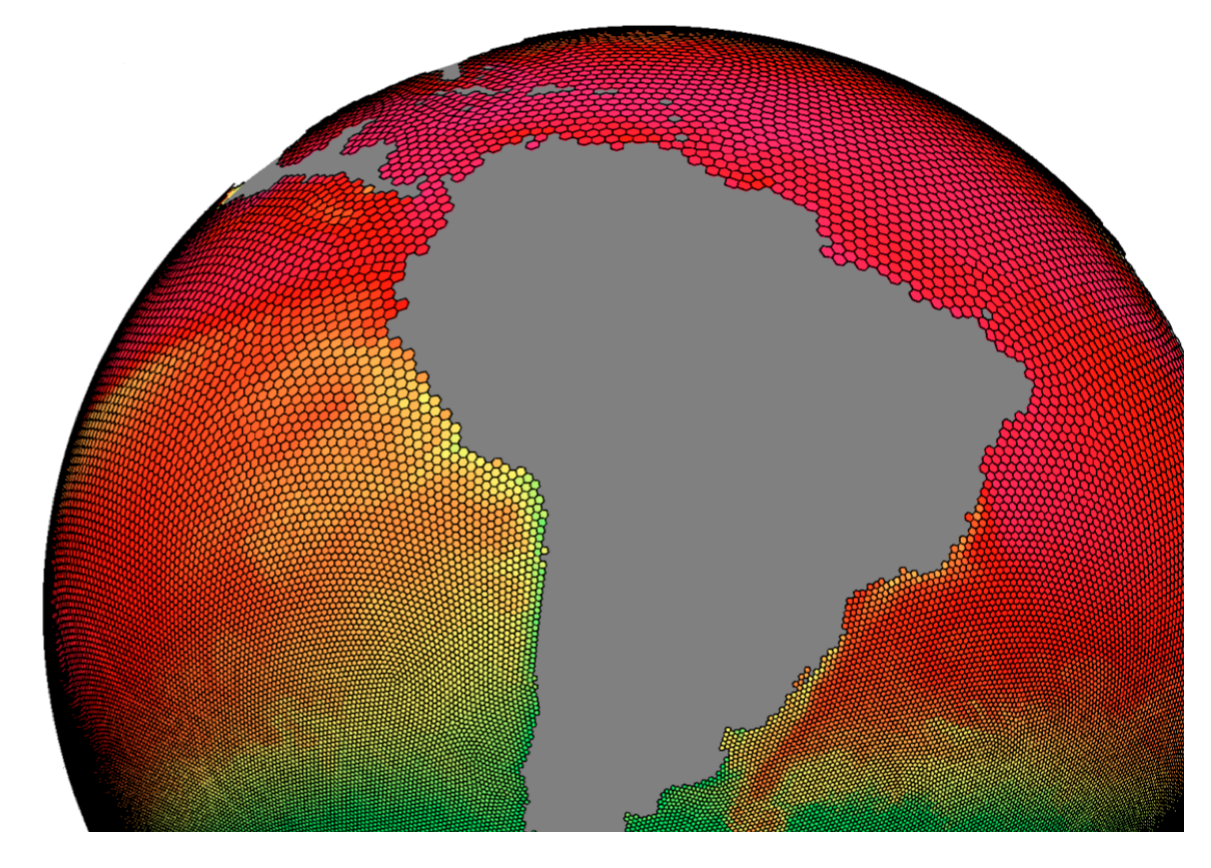
# Simulating Land Ice Evolution within the MPAS Climate Modeling Framework

S.F. Price<sup>1</sup>, M.J. Hoffman<sup>1</sup>, M. Gunzburger<sup>2</sup>, L. Ju<sup>3</sup>, I. Kalashnikova<sup>4</sup>, W. Leng<sup>5</sup>, M. Perego<sup>4</sup>, M. Petersen<sup>1</sup>, T. Ringler<sup>1</sup>, A. Salinger<sup>4</sup>, G. Stadler<sup>5</sup>

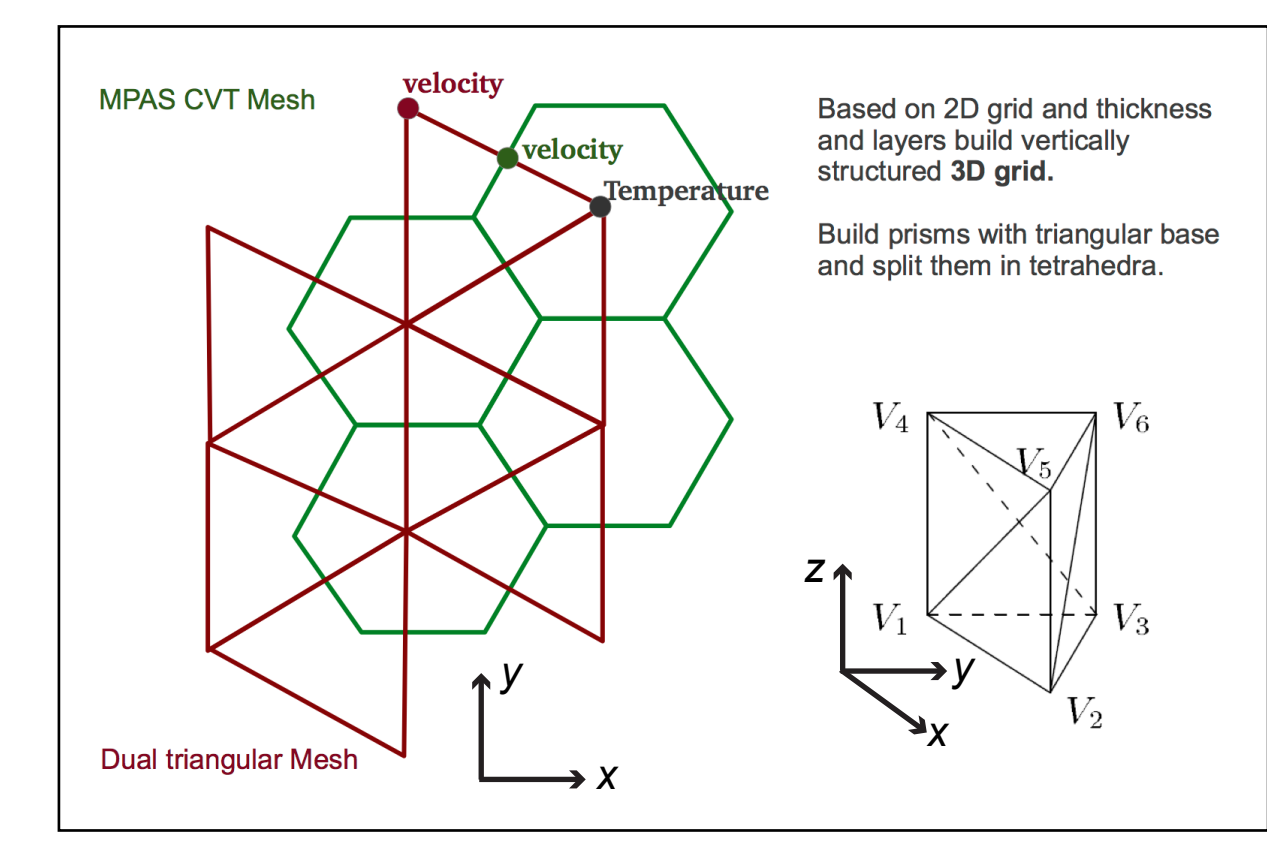
<sup>1</sup>Los Alamos National Laboratory, Los Alamos, NM <sup>2</sup>Florida State University, Tallahassee, FL <sup>3</sup>University of South Carolina, Columbia, SC <sup>4</sup>Sandia National Laboratories, Albuquerque, NM <sup>5</sup>State Key Laboratory, Chinese Academy of Sciences, Beijing, China <sup>6</sup>University of Texas, Austin, TX

## 1. Introduction - Model for Prediction Across Scales (MPAS)

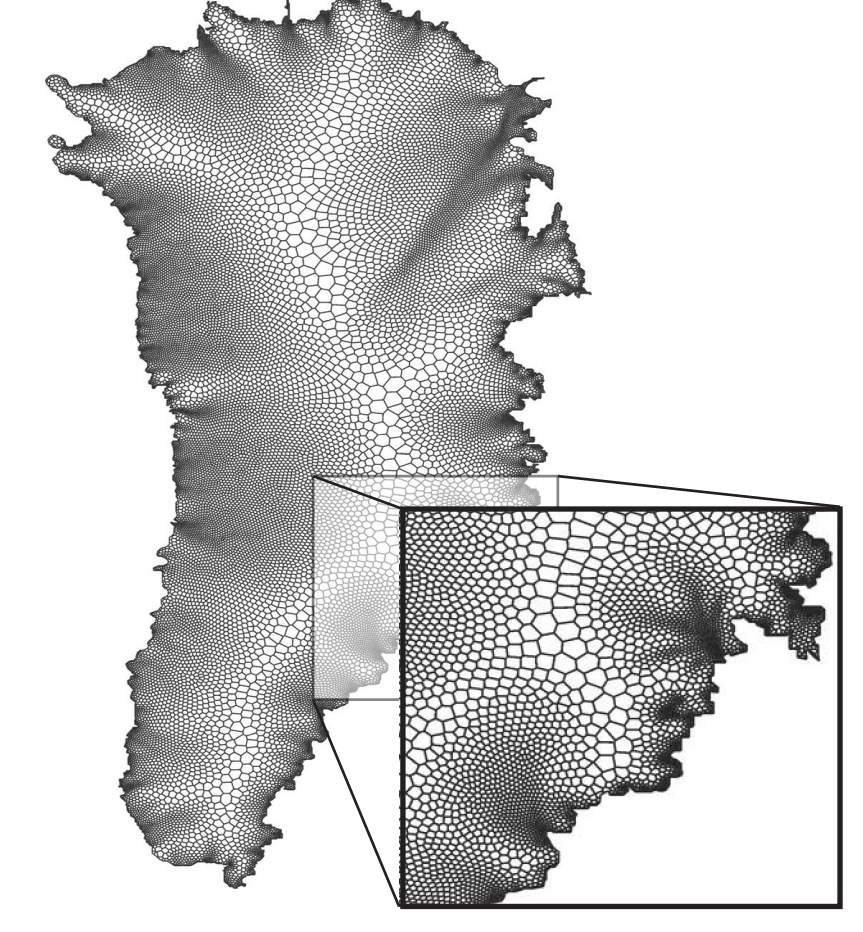
The Model for Prediction Across Scales (MPAS - <http://mpas-dev.github.io>) is a collaborative project for developing atmosphere, ocean and other earth system simulation components for use in climate, regional climate and weather studies. The primary development partners are the climate modeling group at Los Alamos National Laboratory (COSIM) and the National Center for Atmospheric Research. Both partners are responsible for the MPAS framework, operators and tools common to the applications; LANL has primary responsibility for the ocean and land ice models, and NCAR has primary responsibility for the atmospheric model.



MPAS Spherical Centroidal Voronoi Tessellation (SCVT) mesh of the southern ocean, demonstrating a smooth transition from a resolution of 120 km to 30 km cells.



MPAS Centroidal Voronoi Tessellation (CVT) mesh (green polygons) and "dual" triangular mesh (red triangles). The 2d horizontal mesh is extruded in the vertical to build a stack of triangular prisms, which are split into two tetrahedra, appropriate for FEM-based models.



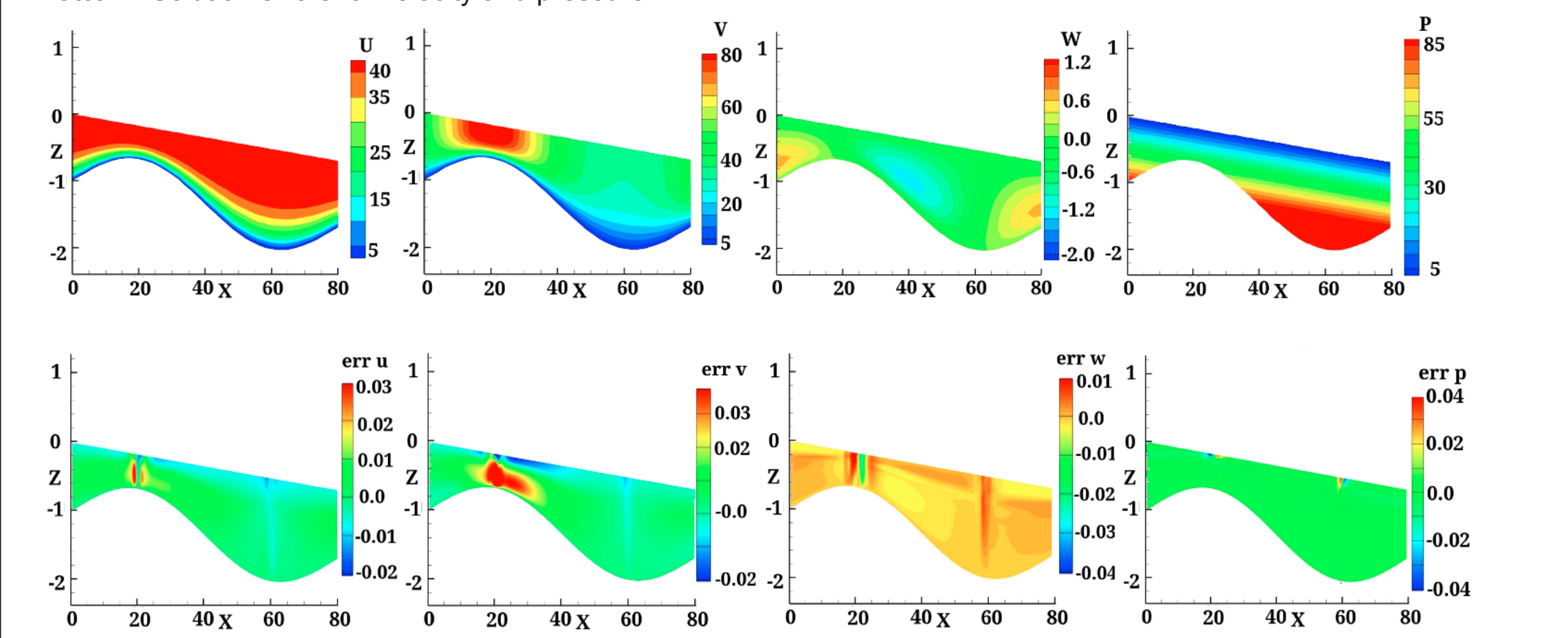
MPAS CVT mesh of Greenland with resolution focused in regions of higher velocity (after Ringler et al., 2008).

The defining features of MPAS are the unstructured Voronoi meshes and C-grid discretization used as the basis for many of the model components. The unstructured Voronoi meshes, formally Spherical Centroidal Voronoi Tessellations (SCVTs), allow for both quasi-uniform discretization of the sphere and local refinement. The C-grid discretization, where the normal component of velocity on cell edges is prognosed, is especially well-suited for higher-resolution, mesoscale atmosphere and ocean simulations. The land ice model takes advantage of the SCVT-dual mesh, which is a triangular Delaunay tessellation appropriate for use with Finite Element Methods (FEM).

## 2. MPAS Land Ice

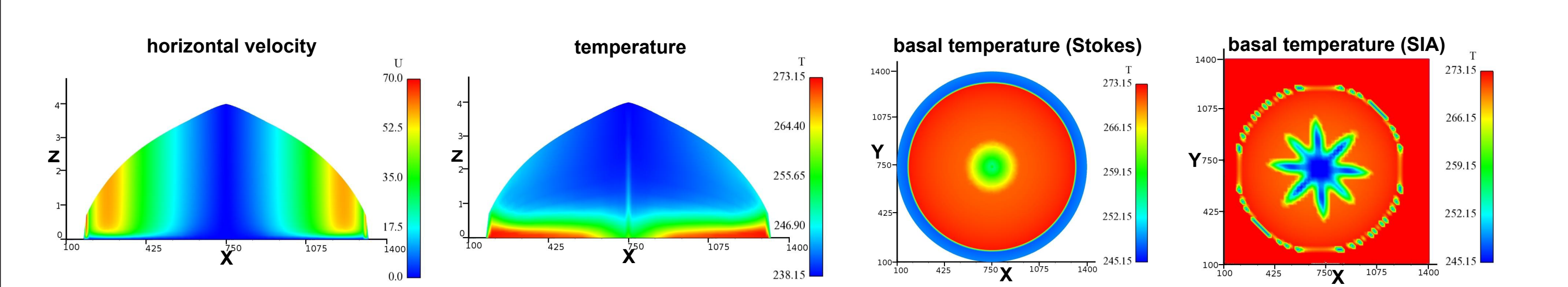
The MPAS Land Ice model currently has access to three dynamical cores. These include nonlinear Stokes (Leng et al., 2012) and 1st-order accurate (Perego et al., 2012; Kalashnikova et al., 2013) dynamical cores, which are FEM-based (FELIX: Finite Elements for Land Ice eXperiments), and a *Fortran90*, native "shallow ice" dynamical core. Verification, performance, and benchmarking of the various dynamical cores is demonstrated in the figures below.

**Top:** Manufactured solutions (Leng et al., 2012) for velocity (u,v,w) and pressure (P) used for verification of FELIX-Stokes. **Bottom:** Solution errors for velocity and pressure.

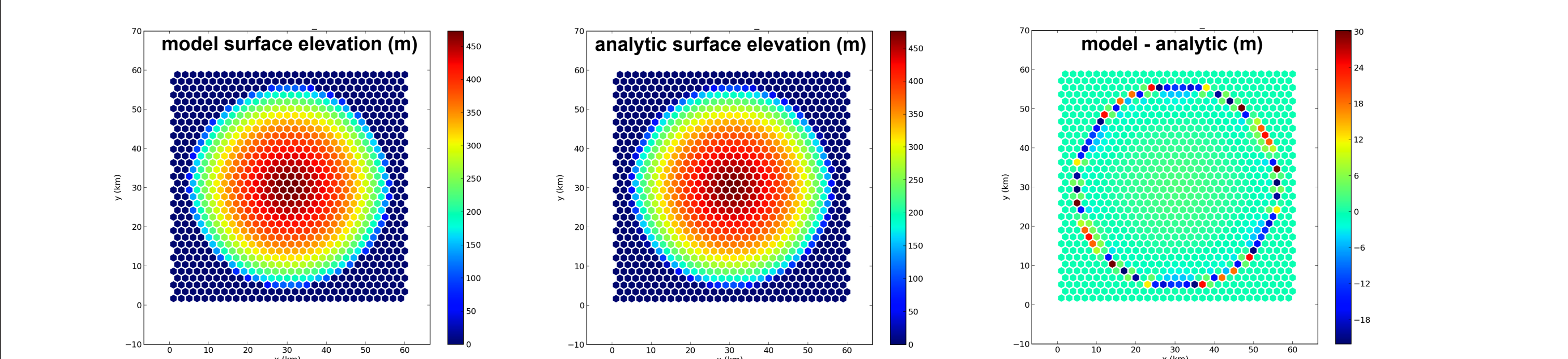


**Right:** Verification of FELIX 1st-order using manufactured solutions. Plots show convergence to analytical solutions with mesh refinement when using finite elements of differing order.

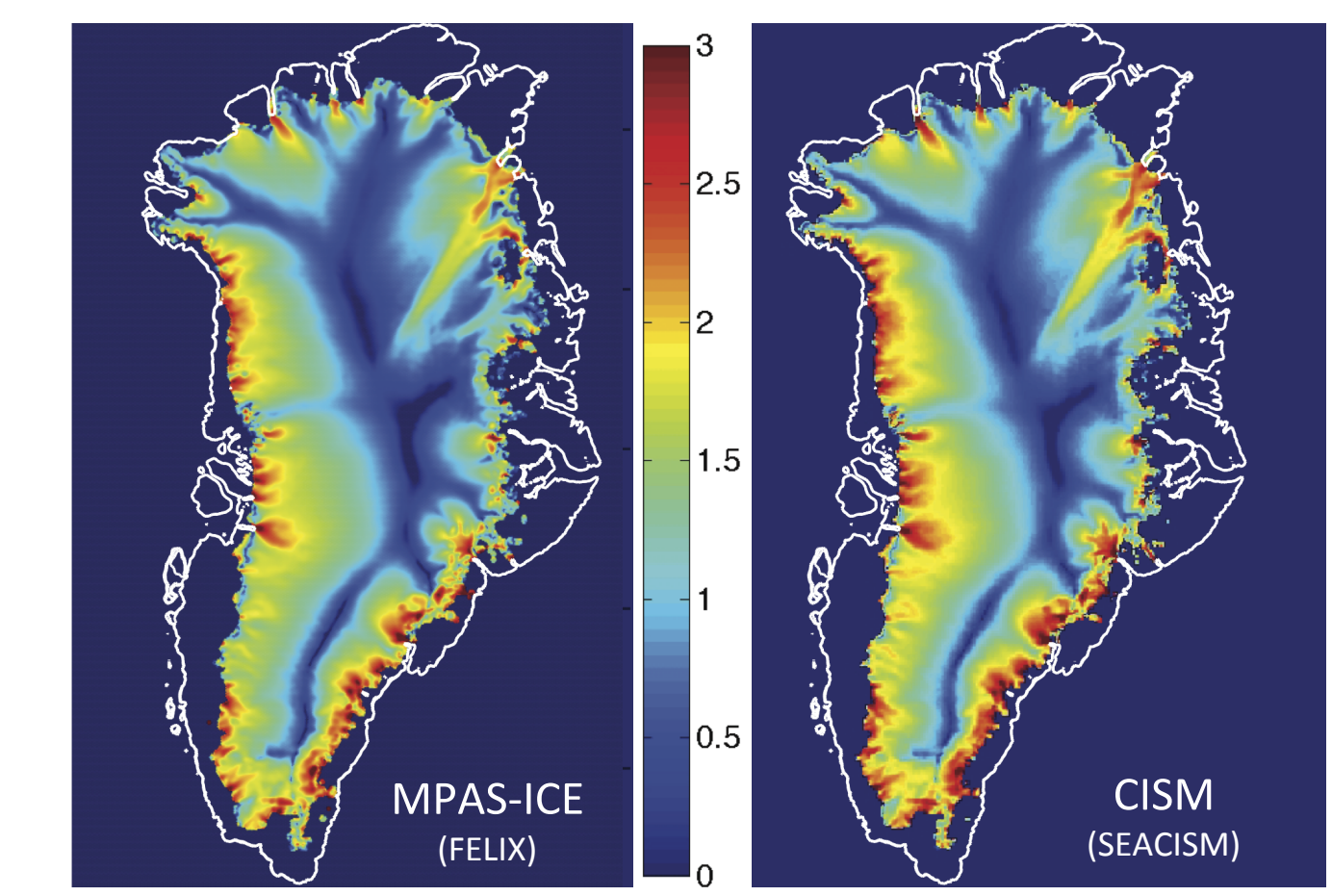
**Below:** Horizontal velocity and temperature with depth and basal temperature at equilibrium for EISMINT II test A (Payne et al., 2000), as calculated from thermomechanically coupled FELIX-Stokes. Note the lack of "cold-spikes" in the basal temperatures (as seen at far-right for SIA model (Rutt et al., 2009)). Additional tests are being conducted to understand if the lack of spikes is due to the FEM discretization, the use of Stokes, or a combination of factors.



**Below:** Analytic (left) and SIA-modeled (middle) solutions for the Halfar test case after  $t=1000$  yrs, and their difference (right).

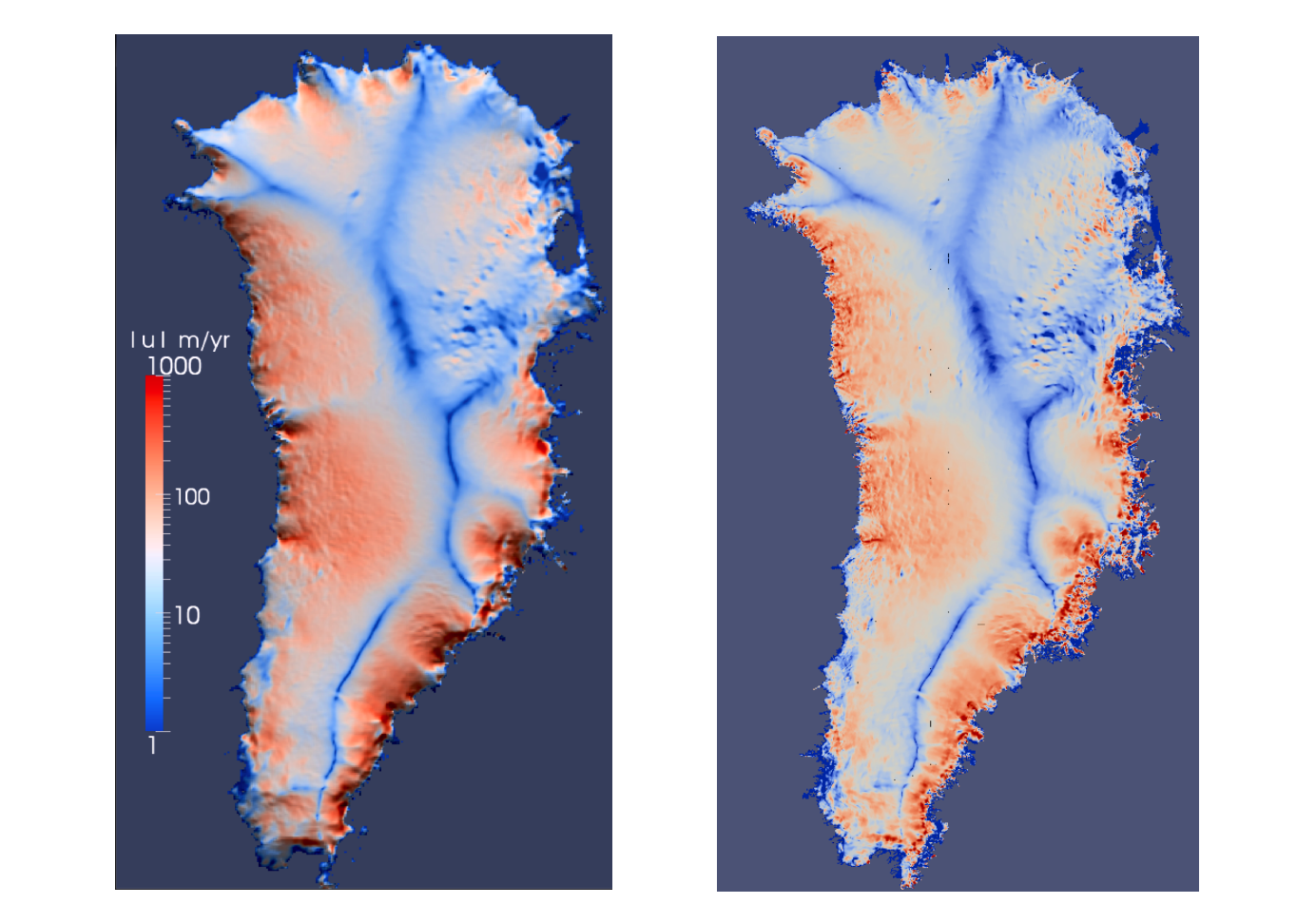


## 3. Application To Realistic Problems



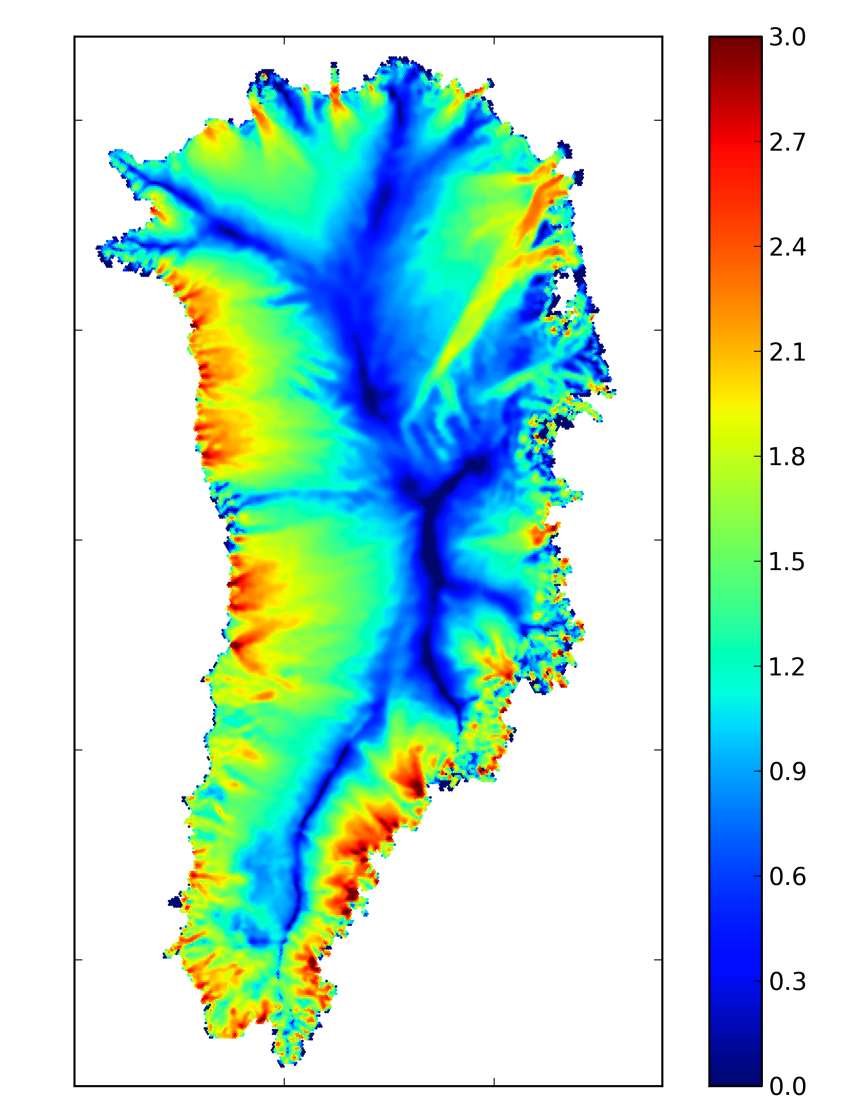
**Left:** Comparison between Greenland surface speed (log10 m/yr) from FELIX 1st-order vs. from the FDM dycore used in Price et al. (2011). Both models use the same tuned basal sliding coefficient field, optimized to match balance velocities.

**Right:** FELIX 1st-order surface speed when optimization attempts to fit observed velocities and a target surface mass balance field, and allows ice thickness to vary within the range of errors from observations (as discussed in more detail in section 4).



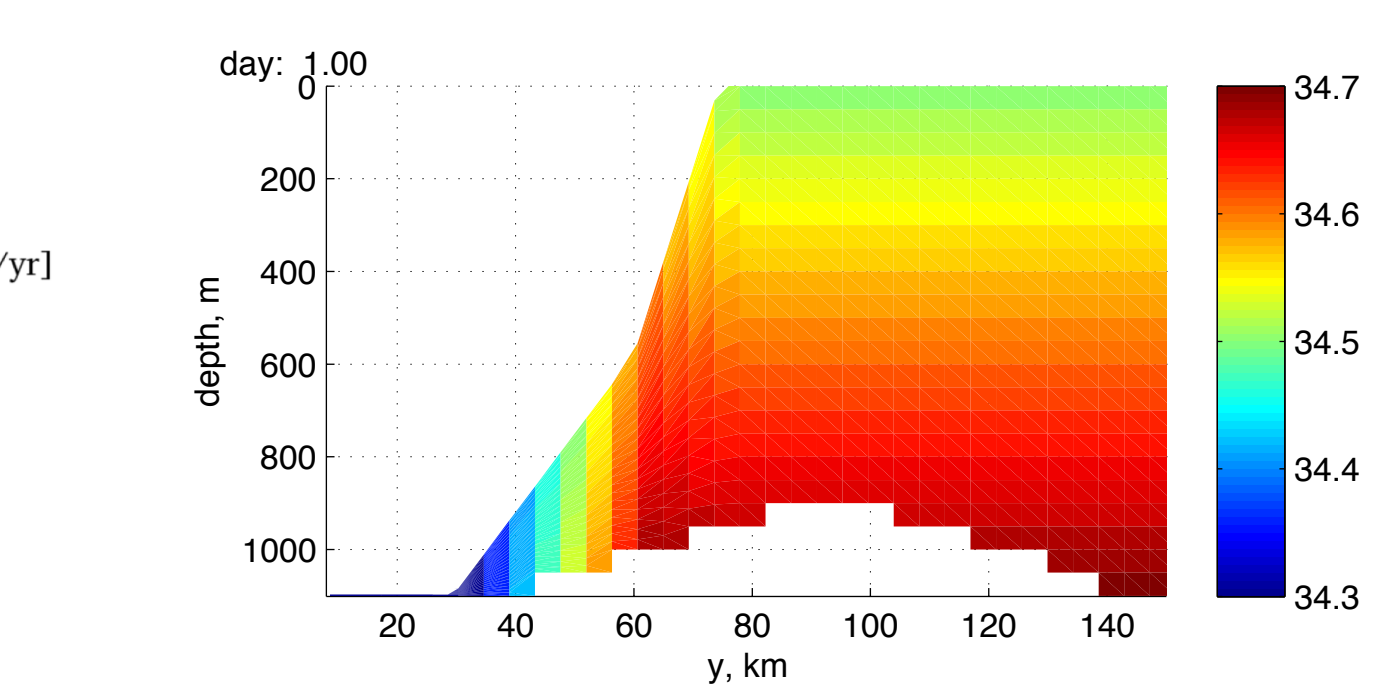
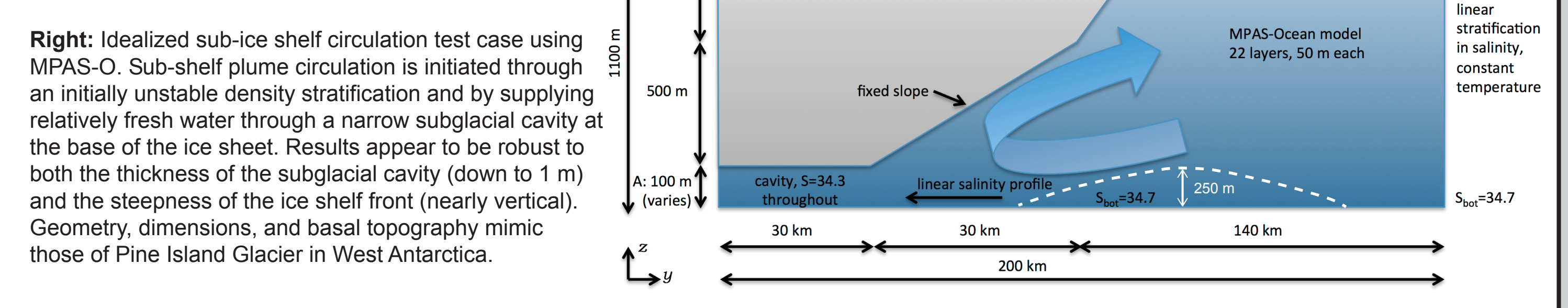
**Left:** Diagnostic surface speed for Greenland (log10 m/yr) from FELIX 1st-order at 5 km (left) and 1 km (right) resolution (no sliding and uniform rate factor assumed).

**Right:** Surface speed for Antarctica (m/yr) calculated from FELIX 1st-order at 10 km resolution with uniform basal sliding coefficient on grounded ice of  $10^5$  Pa yr / m.

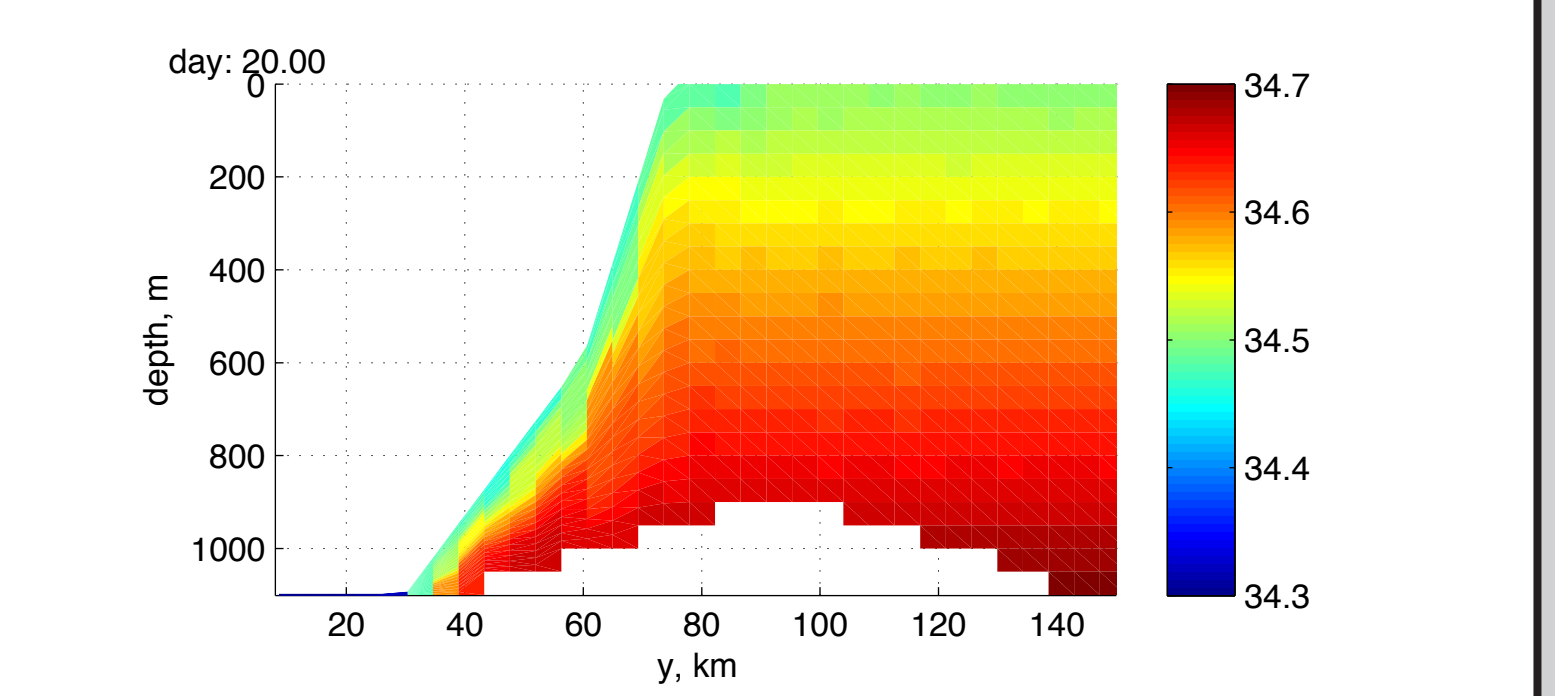


## 5. Ice-Ocean Coupling

Initial tests focused on the ice-ocean coupling capability of the MPAS ocean model (MPAS-O) are very promising. In particular, the vertical coordinate appears to be flexible and robust enough to support arbitrarily large and rapid compression due to the pressure from an overlying ice shelf.



Initial sub-shelf salinity for the idealized test case with a 1 m high subglacial cavity (at  $y=0-30$  km). Other parameters for the problem are detailed in the figure above.



After 20 days of forward model integration, a plot of the sub-shelf salinity indicates turbulent mixing relative to the initial condition and the development of a stable, relatively fresh-water plume circulation beneath the shelf.

## 4. Model Optimization

**Goal:** Find an initial condition such that the ice sheet is at quasi-thermomechanical equilibrium with a given initial geometry (from observations) and surface mass balance (from a climate model) and the mismatch between modeled and observed velocities is minimized. Model parameters that are optimized include the 2d (x,y) fields describing the frictional basal sliding coefficient and the observed ice thickness, which has a specified uncertainty.

$$\frac{\partial H}{\partial t} = -\text{div}(\mathbf{U}H) + \tau_s, \quad \mathbf{U} = \frac{1}{H} \int_z \mathbf{u} dz$$

At equilibrium:  $\text{div}(\mathbf{U}H) = \tau_s$

Basal boundary condition:  $(\sigma_n + \beta \mathbf{u})_{||} = 0 \quad \text{on } \Gamma_\beta$

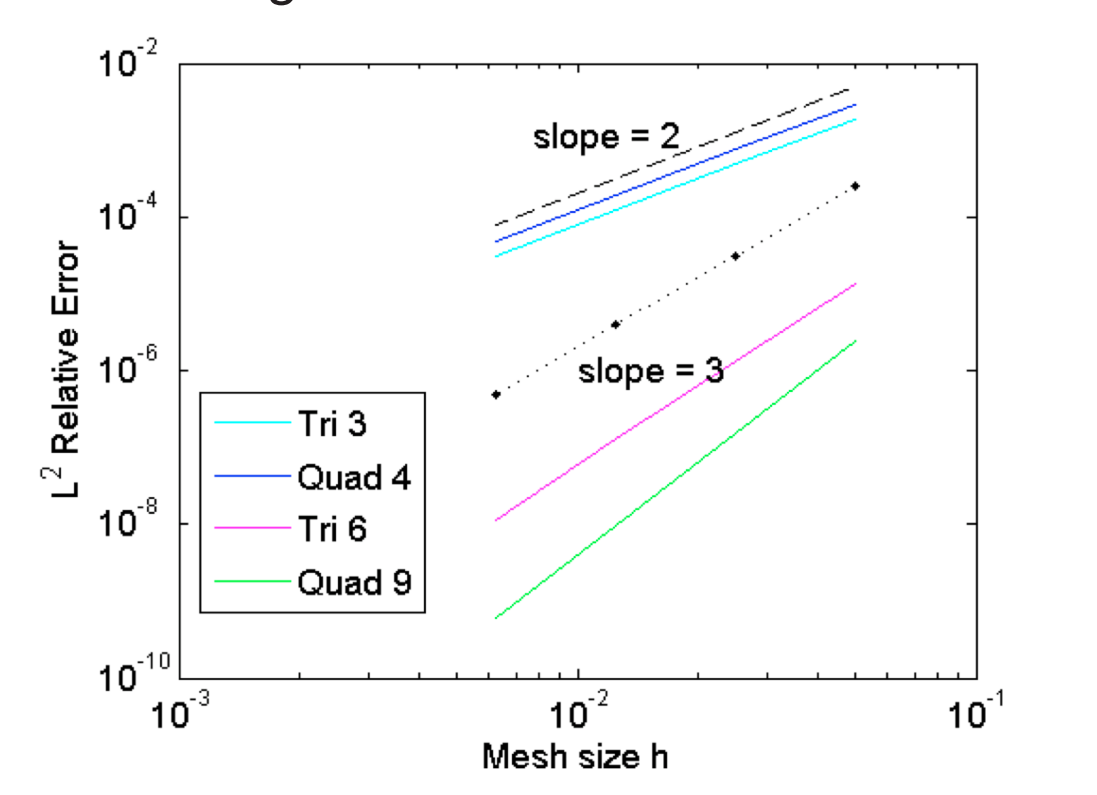
$\mathbf{U}$  : Model depth-averaged velocity  
 $H$  : Ice thickness  
 $\beta$  : Basal sliding coefficient  
 $\tau_s$  : Surface mass balance

The cost function is minimized under the constraint that velocities obey the 1st-order momentum balance with constant ice temperatures. Tikhonov regularization is applied to both the sliding coefficient and the ice thickness. Optimization uses the *Moocho* package from *Trilinos*, applying Sequential Quadratic Programming and LBFGS for approximating the reduced Hessian, to reduce the residual of the constraint (the ice dynamics model) and the cost functional.

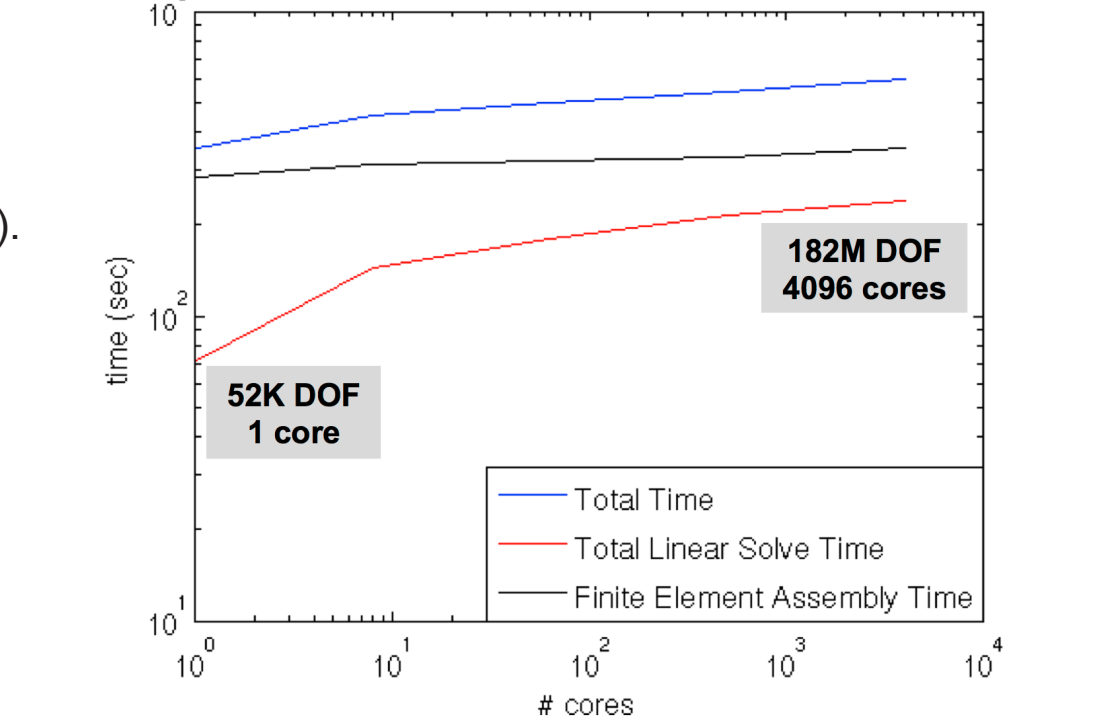
**Optimization Problem:** Find  $\beta$  and  $H$  that minimize the cost functional  $\mathcal{J}$ :

$$\mathcal{J}(\beta, H) = \frac{1}{2} \alpha_d \int_\Gamma |\text{div}(\mathbf{U}H) - \tau_s|^2 ds + \frac{1}{2} \alpha_v \int_{\Gamma_{top}} |\mathbf{u} - \mathbf{u}^{obs}|^2 ds + \frac{1}{2} \alpha_H \int_\Gamma |H - H^{obs}|^2 ds + \mathcal{R}(\beta) + \mathcal{R}(H)$$

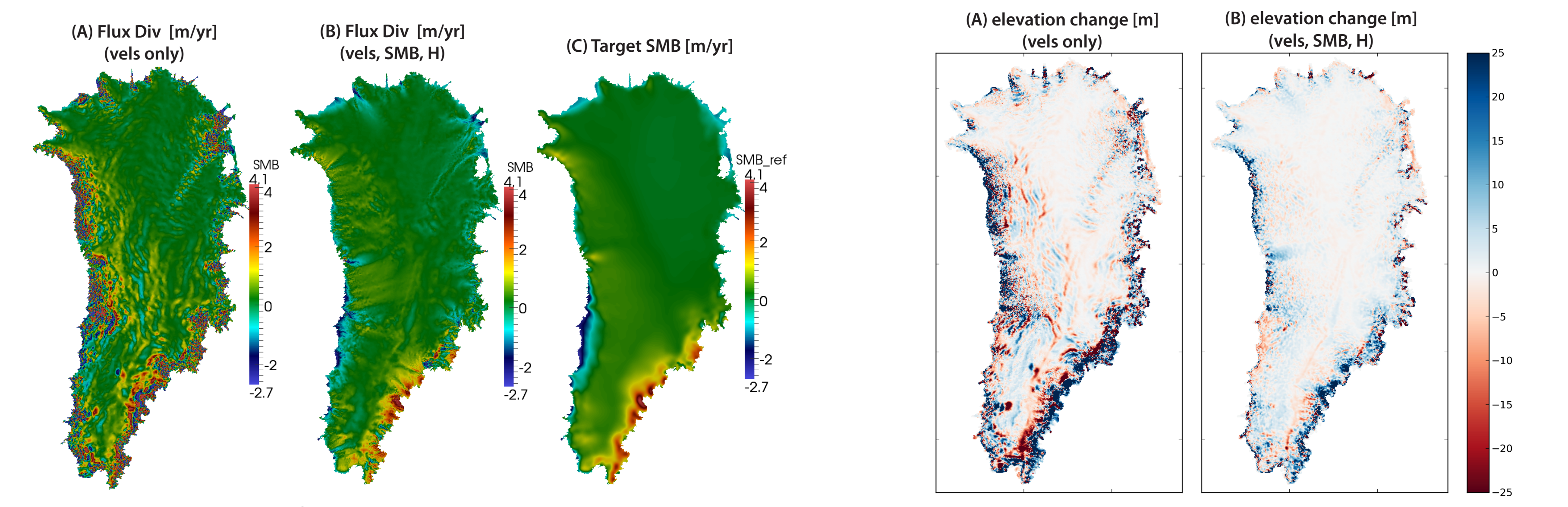
$\int_\Gamma |\text{div}(\mathbf{U}H) - \tau_s|^2 ds$  - flux div. vs. surf. mass bal. mismatch -  
 $\int_{\Gamma_{top}} |\mathbf{u} - \mathbf{u}^{obs}|^2 ds$  - model vs. observed velocity mismatch -  
 $\int_\Gamma |H - H^{obs}|^2 ds$  - model vs. observed thickness mismatch -  
 $\mathcal{R}(\beta) + \mathcal{R}(H)$  - regularization terms -



**Below:** Weak scaling of 1st-order FELIX using ISMIP-HOM test case (Pattyn et al., 2008), showing ~60% efficiency after a 4096x scale-up. Finite element assembly time remains nearly constant.



**Below:** Strong scaling of 1st-order FELIX up to 9k processors, based on diagnostic solve of 2 km resolution Greenland ice sheet test case. 8x processors result in a ~4.5x speedup.

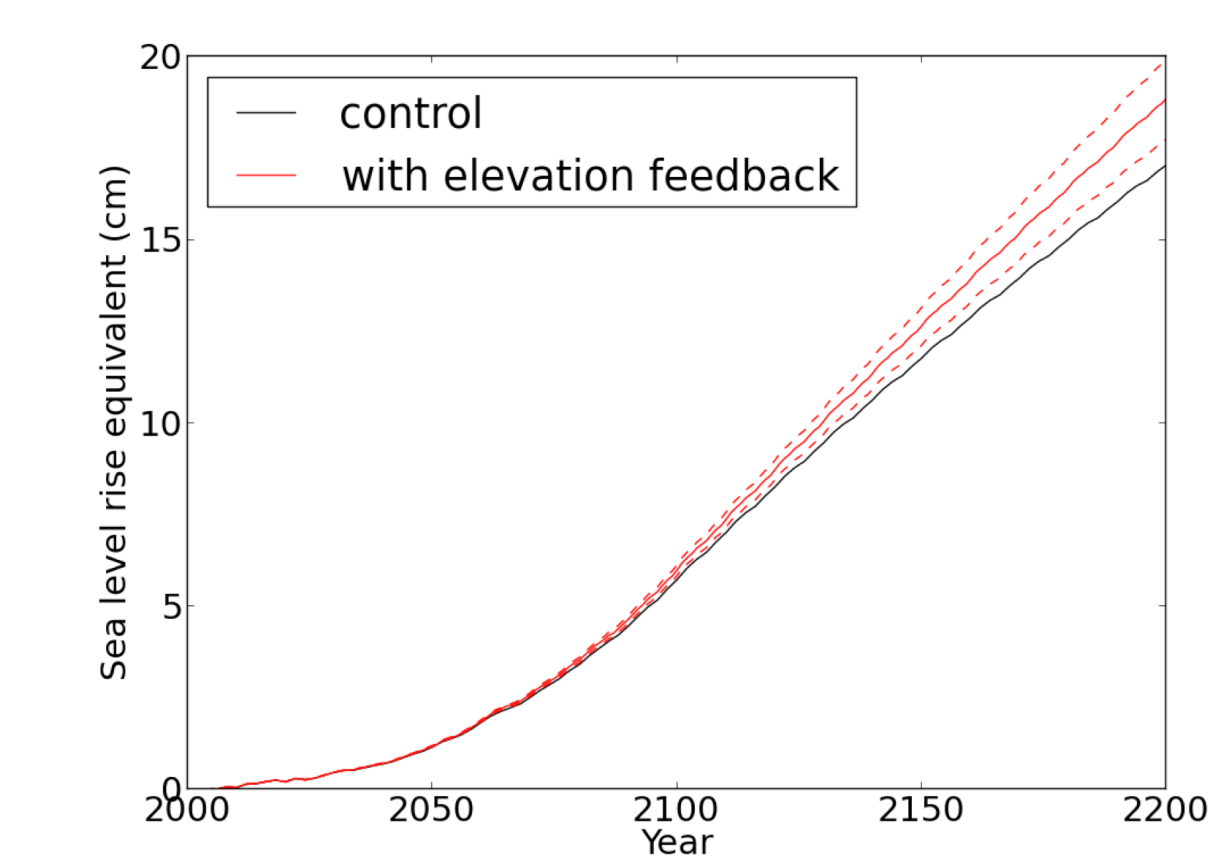


(A) Flux divergence when the cost functional used in optimization includes only the model vs. observed velocity terms and (B) when it also includes the surface mass balance and thickness terms. The "target" surface mass balance, from RACMO, is shown in (C). Note that in (A), the max and min values of several hundreds of m/yr are masked by thresholding of the colorbar.

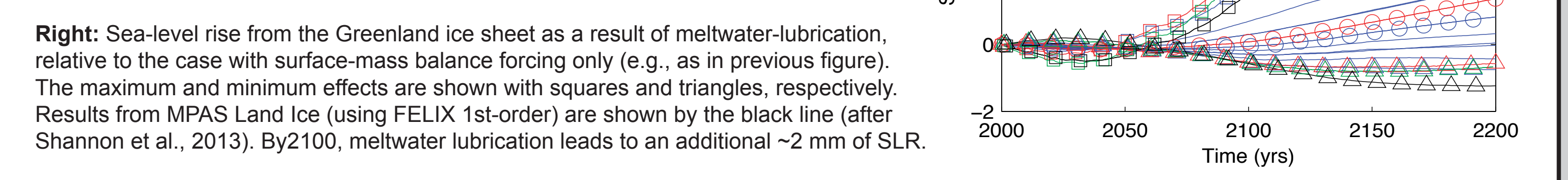
Surface elevation change following ~10 yrs of forward model integration from initial conditions corresponding to panels (A) and (B) in the previous figure. In both cases, the model is forced with the "true" SMB, shown in previous panel (C). For the initial condition optimized to account for the SMB and uncertainties in ice thickness, elevation changes are significantly smaller.

## 6. Science Applications

MPAS Land Ice has been used in Ice2Sea experiments targeted at informing the IPCC AR5 on the potential for sea-level rise from Greenland (Shannon et al., 2013; Edwards et al., 2014a, 2014b).



**Left:** Total sea-level rise from the Greenland ice sheet under the A1B emissions scenario as a result of the feedback between surface elevation, surface temperature, and surface melting (after Edwards et al., 2013b). By 2100, the feedback leads to an additional ~5% of SLR and by 2200 it leads to an additional ~10% of SLR.



**Right:** Sea-level rise from the Greenland ice sheet as a result of meltwater-lubrication, relative to the case with surface-mass balance forcing only (e.g., as in previous figure). The maximum and minimum effects are shown with squares and triangles, respectively. Results from MPAS Land Ice (using FELIX 1st-order) are shown by the black line (after Shannon et al., 2013). By 2100, meltwater lubrication leads to an additional ~2 mm of SLR.

## 8. References

Edwards, T. L., X. Fettweis, O. Gagliardini, F. Gillet-chalet, H. Goelzer, J. M. Gregory, M. Hoffman, P. Huybrechts, A. J. Payne, M. Perego, S. Price, C. Ritz, and A. Quiquet. 2014a. Effect of uncertainty in surface mass balance-elevation feedback on projections of the future sea level contribution of the Greenland ice sheet - Part 1: Parameterisation. *The Cryosphere* (in press).

Edwards, T. L., X. Fettweis, O. Gagliardini, F. Gillet-chalet, H. Goelzer, J. M. Gregory, M. Hoffman, P. Huybrechts, A. J. Payne, M. Perego, S. Price, C. Ritz, and A. Quiquet. 2014b. Effect of uncertainty in surface mass balance-elevation feedback on projections of the future sea level contribution of the Greenland ice sheet - Part 2: Projections. *The Cryosphere* (in press).

Kalashnikova, I., D. F. Martin, S. F. Price et al. 2013. Ice sheet model dynamical core development for PISCES. DOE SciDAC PI meeting, Rockville, MD, July 2013.

Leng, W., L. Ju, M. Gunzburger, S. F. Price, and T. Ringler. 2012. A Parallel High-Order Accurate Finite Element Nonlinear Stokes Ice-Sheet Model and Benchmark Experiments. *J. Geophys. Res.*, 117.

Pattyn, F. et al. 2008. Benchmark experiments for higher-order and full Stokes ice sheet models (ISMIP-HOM). *The Cryosphere Discussions* 2, 111-151.

Payne, A. J. et al. Results from the EISMINT model intercomparison: the effects of thermomechanical coupling. *J. Glaciol.* 46, 227-238 (2000).

Perego, M., M. Gunzburger, and J. Burkardt. 2012. Parallel finite element implementation of higher-order ice sheet models. *J. Glaciol.*, 58, 76-88.

Price, S. F., A. J. Payne, I. M. Howat, and B. E. Smith. 2011. Committed sea-level rise for the next century from Greenland ice sheet dynamics during the past decade. *PNAS*. doi:10.1073/pnas.1017131108.

Ringler, T., L. Ju and M. Gunzburger. 2008. A multiresolution method for climate system modeling: application of spherical centroidal Voronoi tessellations. *Ocean Dynamics*, 58 (5-6), 475-498.

Rutt, I., Hagdorn, M., Hulton, N. & Payne, A. 2009. The Glimmer community ice sheet model. *J. Geophys. Res.* 114, F02004.

Shannon, S. R., A. J. Payne, I. D. Bartholomew, M. R. van den Broeke, T. L. Edwards, X. Fettweis, O. Gagliardini, F. Gillet Chalet, H. Goelzer, M. J. Hoffman, P. Huybrechts, D. Mair, P. Nienow, M. Perego, S. F. Price, C. J. PPSmeets, A. J. Sole, R. S. W. van de Wal and T. Zwinger. 2013. Enhanced basal lubrication and the contribution of the Greenland ice sheet to future sea level rise. *PNAS*. doi:10.1073/pnas.1212647110.